



Variants in *TRIM22* That Affect NOD2 Signaling Are Associated With Very-Early-Onset Inflammatory Bowel Disease

Qi Li,^{1,2,*} Cheng Hiang Lee,^{3,4,*} Lauren A. Peters,^{5,6,*} Lucas A. Mastropaolo,² Cornelia Thoeni,^{1,2} Abdul Elkadri,^{1,2,7} Tobias Schwerd,⁸ Jun Zhu,⁶ Bin Zhang,⁶ Yongzhong Zhao,⁶ Ke Hao,⁶ Antonio Dinarzo,⁶ Gabriel Hoffman,⁶ Brian A. Kidd,⁶ Ryan Murchie,^{1,2} Ziad Al Adham,^{1,2,7} Conghui Guo,² Daniel Kotlarz,⁹ Ernest Cutz,¹⁰ Thomas D. Walters,^{1,2} Dror S. Shouval,¹¹ Mark Curran,¹² Radu Dobrin,¹² Carrie Brodmerkel,¹² Scott B. Snapper,^{11,13} Christoph Klein,⁹ John H. Brumell,^{1,7,14} Mingjing Hu,^{3,4} Ralph Nanan,^{3,4} Brigitte Snanter-Nanan,^{3,4} Melanie Wong,¹⁵ Francoise Le Deist,¹⁶ Elie Haddad,¹⁷ Chaim M. Roifman,¹⁸ Colette Deslandres,¹⁹ Anne M. Griffiths,^{1,2} Kevin J. Gaskin,^{3,4} Holm H. Uhlig,⁸ Eric E. Schadt,^{6,§} and Aleixo M. Muişe^{1,2,7,§}

¹SickKids Inflammatory Bowel Disease Center and Cell Biology Program, Research Institute, Hospital for Sick Children, Toronto, Ontario, Canada; ²Division of Gastroenterology, Hepatology, and Nutrition, Department of Pediatrics, University of Toronto, Hospital for Sick Children, Toronto, Ontario, Canada; ³Gastroenterology Department, The Children's Hospital at Westmead, Westmead, New South Wales, Australia; ⁴The James Fairfax Institute of Paediatric Nutrition, University of Sydney, New South Wales, Australia; ⁵Graduate School of Biomedical Sciences, Icahn School of Medicine at Mount Sinai, New York, New York; ⁶Department of Genetics and Genomic Sciences, Icahn School of Medicine at Mount Sinai and the Icahn Institute for Genomics and Multiscale Biology, New York, New York; ⁷Institute of Medical Science, University of Toronto, Toronto, Ontario, Canada; ⁸Translational Gastroenterology Unit, Nuffield Department of Clinical Medicine, Experimental Medicine Division, University of Oxford and Department of Pediatrics, John Radcliffe Hospital, Oxford, UK; ⁹Department of Pediatrics, Dr. von Hauner Children's Hospital, Ludwig-Maximilians-University, Munich, Germany; ¹⁰Division of Pathology, The Hospital for Sick Children, Toronto, Ontario, Canada; ¹¹Division of Pediatric Gastroenterology, Hepatology, and Nutrition, Department of Pediatrics, Boston Children's Hospital, Harvard Medical School, Boston, Massachusetts; ¹²Janssen R&D, LLC, Spring House, Pennsylvania; ¹³Division of Gastroenterology and Hepatology, Brigham & Women's Hospital, Department of Medicine, Boston, Massachusetts; ¹⁴Molecular Genetics, University of Toronto, Toronto, Ontario, Canada; ¹⁵Immunology Department, The Children's Hospital at Westmead, Westmead, New South Wales, Australia; ¹⁶Department of Microbiology and Immunology, CHU Sainte Justine and Department of Microbiology, Infectiology and Immunology, University of Montreal, Quebec, Canada; ¹⁷Department of Pediatrics, CHU Sainte-Justine, Department of Microbiology, Infectiology and Immunology, University of Montreal, Quebec, Canada; ¹⁸Division of Immunology, Department of Pediatrics, University of Toronto, The Hospital for Sick Children, Toronto, Canada; and ¹⁹Division of Gastroenterology, Hepatology and Nutrition, Department of Pediatrics, CHU Sainte-Justine, Montreal, Quebec, Canada

See Covering the Cover synopsis on page 1050.

BACKGROUND & AIMS: Severe forms of inflammatory bowel disease (IBD) that develop in very young children can be caused by variants in a single gene. We performed whole-exome sequence (WES) analysis to identify genetic factors that might cause granulomatous colitis and severe perianal disease, with recurrent bacterial and viral infections, in an infant of consanguineous parents. **METHODS:** We performed targeted WES analysis of DNA collected from the patient and her parents. We validated our findings by a similar analysis of DNA from 150 patients with very-early-onset IBD not associated with known genetic factors analyzed in Toronto, Oxford, and Munich. We compared gene expression signatures in

inflamed vs noninflamed intestinal and rectal tissues collected from patients with treatment-resistant Crohn's disease who participated in a trial of ustekinumab. We performed functional studies of identified variants in primary cells from patients and cell culture. **RESULTS:** We identified a homozygous variant in the tripartite motif containing 22 gene (*TRIM22*) of the patient, as well as in 2 patients with a disease similar phenotype. Functional studies showed that the variant disrupted the ability of TRIM22 to regulate nucleotide binding oligomerization domain containing 2 (NOD2)-dependent activation of interferon-beta signaling and nuclear factor- κ B. Computational studies demonstrated a correlation between the TRIM22-NOD2 network and signaling pathways and genetic factors associated very early onset and adult-onset IBD. TRIM22 is also associated with antiviral and mycobacterial

*Authors share co-first authorship; §Authors share co-senior authorship.

Abbreviations used in this paper: eQTL, expression quantitative trait loci; GWAS, genome-wide association study; MDP, muramyl dipeptide; NF- κ B, nuclear factor- κ B; NOD2, nucleotide binding oligomerization domain containing 2; RSV, to respiratory syncytial virus; TNF, tumor necrosis

factor; TRIM22, tripartite motif containing 22 gene; VEOIBD, Very-early-onset inflammatory bowel diseases; WES, whole exome sequencing.

Most current article

© 2016 by the AGA Institute Open access under CC BY-NC-ND license. 0016-5085

<http://dx.doi.org/10.1053/j.gastro.2016.01.031>

effectors and markers of inflammation, such as fecal calprotectin, C-reactive protein, and Crohn's disease activity index scores. **CONCLUSIONS:** In WES and targeted exome sequence analyses of an infant with severe IBD characterized by granulomatous colitis and severe perianal disease, we identified a homozygous variant of *TRIM22* that affects the ability of its product to regulate NOD2. Combined computational and functional studies showed that the *TRIM22-NOD2* network regulates antiviral and antibacterial signaling pathways that contribute to inflammation. Further study of this network could lead to new disease markers and therapeutic targets for patients with very early and adult-onset IBD.

Keywords: VEOIBD; NF- κ B; Antiviral and Antibacterial Networks.

Very-early-onset inflammatory bowel diseases (VEOIBD) often present with severe multisystemic disease that is difficult to treat with conventional therapies. These young patients frequently have novel causal¹⁻³ and risk variants⁴⁻⁸ and common networks are now being established (reviewed in Uhlig et al⁹). For example, mutations in *IL10RA/B* genes cause a Mendelian form of VEOIBD with severe colitis and perianal disease¹⁰ and mutations in *TTC7A* cause a severe form of apoptotic enterocolitis.¹

Tripartite motif-containing 22 (*TRIM22*; also known as *STAF50*) is a RING finger E3 ubiquitin ligase¹¹ that is expressed in the intestine¹² and in macrophages,¹³ and has a role in lineage-specific differentiation of lymphocytes.¹⁴ *TRIM22* was originally identified as an interferon inducible protein that possesses antiviral activity¹⁵⁻¹⁷ and activates nuclear factor- κ B (NF- κ B) signaling.¹³ Here we identify *TRIM22* functional variants associated with a distinct VEOIBD phenotype characterized by granulomatous colitis and severe perianal disease and show the *TRIM22-NOD2* network as a key antiviral and mycobacterial regulator.

Materials and Methods

See [Supplementary Material](#) for full methods information.

Subjects

All experiments were carried out with the approval of the Research Ethics Board at the Hospital for Sick Children. Informed consent to participate in research was obtained. A copy of the consent is available on the NEOPICS (International Early Onset Pediatric IBD Cohort Study) website (http://www.neopics.org/NEOPICS_Documents.html).

Whole Exome Sequencing

For patient 1 and her parents (trio), whole exome sequencing (WES) was performed using the Agilent SureSelect Human All Exon 50-Mb kit with high-throughput sequencing conducted using the SOLiD 4 System at The Center for Applied Genomics through the Hospital for Sick Children (Toronto). Sanger sequencing was used to verify variant genotypes in family 1 and infantile patients from the collaborating institutions were screened for *TRIM22* variants.

Validation

In order to validate these findings, we examined WES results from 150 infantile international VEOIBD patients without a genetic diagnosis who were previously sequenced in Toronto (NEOPICS), Oxford, and Munich (Care for Rare) and targeted exome sequencing of the *TRIM22* gene in 10 *IL10RA/B*, and *IL10*-negative patients without previous WES.

Computational Analysis

Datasets. Biopsy data were collected at baseline from anti-tumor necrosis factor (TNF)-resistant Crohn's patients enrolled in the ustekinumab trial described previously.¹⁸ The ustekinumab trial expression data were used for construction of the adult IBD network. RNA-seq from the RISK cohort, as described previously,¹⁹ was used for generation of the pediatric IBD Bayesian network.

Differential expression. To ascertain tissue-specific signatures, we examined inflamed vs noninflamed tissue from various anatomic regions of the small intestine, colon, and rectum. To identify differential expression signatures, we used an unbiased univariate filter to select top-varying genes and then applied Significance Analysis of Microarrays²⁰ (SAM) to whole-genome expression data collected from biopsy tissue samples and whole blood of individuals in the ustekinumab trial. To control for multiple hypothesis testing, we used the Benjamini & Hochberg adjustment on the raw *P* values to control the family-wise error rate and set a false discovery rate threshold of 1% or 5%. All analyses were performed using the R statistical package, version 2.15.24.1

Bayesian network. We employed Monte Carlo Markov Chain²¹ simulation to identify potentially thousands of different plausible networks that are then combined to obtain a consensus network. eSNP data were used as priors as follows: genes with cis-eSNP²² are allowed to be parent nodes of genes without cis-eSNPs, but genes without cis-eSNPs are not allowed to be parents of genes with cis-eSNPs.

Key driver analysis. Key driver analysis takes as input a set of genes (*G*) and a directed gene network (*N*) (eg, Bayesian network).^{19,23-26} The objective is to identify the key regulators for the gene sets with respect to the given network. Key driver analysis first generates a subnetwork N_G , defined as the set of nodes in *N* that are no more than *h*-layers away from the nodes in *G*, and then searches the *h*-layer neighborhood ($h = 1, \dots, H$) for each gene in N_G ($HLN_{g,h}$) for the optimal h^* , such that

$$ES_{h^*} = \max (ES_{h,g}) \forall g \in N_g, h \in \{1 \dots H\}$$

where $ES_{h,g}$ is the computed enrichment statistic for $HLN_{g,h}$. A node becomes a candidate driver if its HLN is significantly enriched for the nodes in *G*. Candidate drivers without any parent node (ie, root nodes in directed networks) are designated as global drivers, while the remaining are designated as local drivers.

Pathway enrichment. Expression quantitative trait loci (eQTL) analysis was performed on IBD, ulcerative colitis, and Crohn's disease genome-wide association study (GWAS) hits from the National Human Genome Research Institute catalog, plus all Wellcome Trust Case Control Consortium IBD GWAS single nucleotide polymorphisms with $P \leq .001$. Ten percent false discovery rate eGenes were thus extracted, and tested for enrichment of pathways from the Metacore database.

Clinical variable correlation. We used Spearman correlation to examine the relationship between the messenger RNA expression of *TRIM22* in intestine and blood and several key IBD traits. The correlation test was performed with the R function “corr.test.” We applied a simple Bonferroni correction to a .01 significance level across all gene-trait correlation tests performed.

Transfection and luciferase reporter assays. NF- κ B luciferase reporter plasmids (Promega, Madison, WI) and interferon-stimulated response element promoter and interferon-beta promoter luciferase reporter plasmids were obtained from Dr Hong-bing Shu (Wuhan University). A total of HEK 293 cells (1×10^5) were seeded on 24-well dishes and transfected the following day using Lipofectamine 2000 method. Empty control plasmid was added to ensure that each transfection received the same amount of total DNA. To normalize for transfection efficiency, 0.01 μ g pRL-TK (Renilla luciferase) reporter plasmid was added to each transfection. Approximately 24 hours after transfection, luciferase assays were performed using a dual-specific luciferase assay kit (Promega). Firefly luciferase activities were normalized on the basis of Renilla luciferase activities. Cells were treated with recombinant TNF α , respiratory syncytial virus (RSV), or L18-muramyl dipeptide (MDP) (InvivoGen, San Diego, CA). Statistical analysis of luciferase assay data consisted of 2-way analysis of variance followed by Bonferroni post-hoc testing to compare across conditions. Statistical significance was assigned to tests with $P < .05$ after Bonferroni correction.

Coimmunoprecipitation and immunoblot analysis. For transient transfection and coimmunoprecipitation experiments, HEK 293 cells (1×10^6) were seeded for 24 hours then transiently transfected for 18 to 24 hours using Lipofectamine 2000 according to the manufacturer's protocols. Transfected cells were lysed in 1 mL lysis buffer (150 mM NaCl, 50 mM HEPES, 1% Triton X-100, 10% glycerol, 1.5 mM MgCl₂, 1.0 mM ethylene glycol-bis[β -aminoethyl ether]-*N,N,N',N'*-tetraacetic acid) supplemented with protease and phosphatase inhibitors (aprotinin, 1:1000; leupeptin, 1:1000; pepsin, 1:1000; and phenylmethylsulfonyl fluoride, 1:100). For each immunoprecipitation, a 0.9-mL aliquot of the lysate was incubated with 0.5 μ L of the indicated antibody and 40 μ L of a 1:1 slurry of Protein G Sepharose (Bioshop, Burlington, ON, Canada) for 1 hour. Sepharose beads were washed 3 \times with 1 mL high salt lysis buffer containing 0.5 M NaCl. The precipitates were analyzed by standard immunoblot procedures using the following antibodies: mouse monoclonal anti-FLAG (Sigma, St Louis, MA), anti-HA (Origene, Rockville, MD), anti-NOD2 (Novus), anti-green fluorescent protein (Invitrogen, Carlsbad, CA), rabbit polyclonal anti-TRIM22 (Abnova, Taipei City, Taiwan), and goat polyclonal anti-NOD2 (Ingenix). For endogenous coimmunoprecipitation experiments, HT29 cells (5×10^7) were stimulated with MDP (10 μ g/mL) for the indicated times or left untreated. The coimmunoprecipitation and immunoblot experiments were performed as described here.

Results

Case History

Patient 1 was born in Australia to consanguineous parents. She initially presented on day 8 of life with fever, oral ulcers, diarrhea, and failure to thrive and later developed

severe fistulizing perianal disease (Figure 1A) and granulomatous colitis (Figure 1B). She deteriorated despite treatment with corticosteroid and biologic therapy. Symptomatic control was only achieved by fecal stream diversion with combined ileostomy and subtotal colectomy. Patients 2 and 3 had a very similar clinical course, with granulomatous colitis and severe perianal disease (Figure 1C and D) requiring ileostomy followed by total proctocolectomy. Both patients 2 and 3 presented with severe anemia and severe hypoalbuminemia secondary to colitis. Patients 1 and 2 had numerous bacterial and viral infections. The 3 patients did not have mutations in the *IL10RA/B*, *IL10*, *XIAP*, or *NOD2* genes, and were all very difficult to treat medically and surgically, with their disease nonresponsive to anti-TNF α biologic therapy (Supplementary Table 1A; see Supplementary Material for full clinical description).

Whole Exome Sequencing

WES of patient 1 (and parents) resulted in $>100\times$ the mean exome coverage and identified 152,020 variants, including 16,097 rare variants (minor allelic frequency <0.01) predicted to be damaging (Supplementary Figure 1). From this list, we identified 12 nonsynonymous homozygous variants (Supplementary Table 2) that were inherited in an autosomal recessive manner. Based on known protein function, expression profiles, animal models, mutation conservation, and network analysis. This list was narrowed down to a single candidate gene—*TRIM22*. Patient 1 had a homozygous nonsynonymous variant in exon 7 of the *TRIM22* gene inherited from both parents (Figure 1E). This missense variant resulted in an arginine to cysteine substitution (c.1324C>T; p.Arg442Cys) predicted to be highly deleterious (Figure 1F and Supplementary Table 1B). It is highly conserved in a functionally significant region of the exposed beta sheet around the variable loop 3 (V3) in the B30.2 (SPRY) domain thought to be responsible for subcellular localization^{27,28} and the 3-dimensional structure suggest it results in an elongated or additional beta strand, which in the wild type, forms a relaxed loop segment.

To validate, we examined WES from 150 VEOIBD patients, but did not identify damaging variants in *TRIM22*. Therefore, we performed targeted exome sequencing in 10 patients with a similar severe phenotype and identified 2 additional patients with *TRIM22* variants (patients 2 and 3). Patient 2 had compound heterozygous *TRIM22* variants (Figure 1E), including a novel arginine to threonine substitution (c.449G>C, p.Arg150Thr) inherited paternally; and a serine to leucine substitution (c.731C>T; p.Ser244Leu) inherited maternally. Both variants were predicted to be damaging and to disrupt the highly conserved coiled-coil region of TRIM22 that facilitates homodimer/heterodimer multimers (Figures 1F, Supplementary Figure 2, and Supplementary Table 1B). R150T is in an exposed region and S244L is buried and resides in the spacer-2 region that contains a bipartite nuclear localization sequence, and was previously predicted to be a serine phosphorylation site.²⁷

Patient 3 had a homozygous *TRIM22* variant inherited from both parents (Figure 1E). This nonsynonymous variant

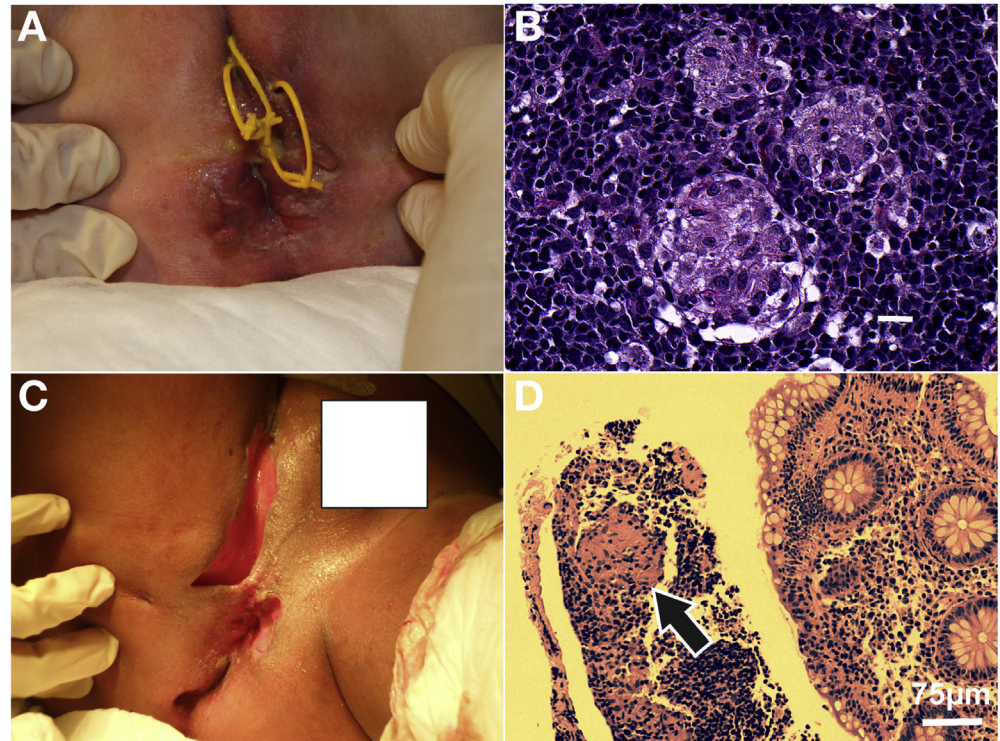
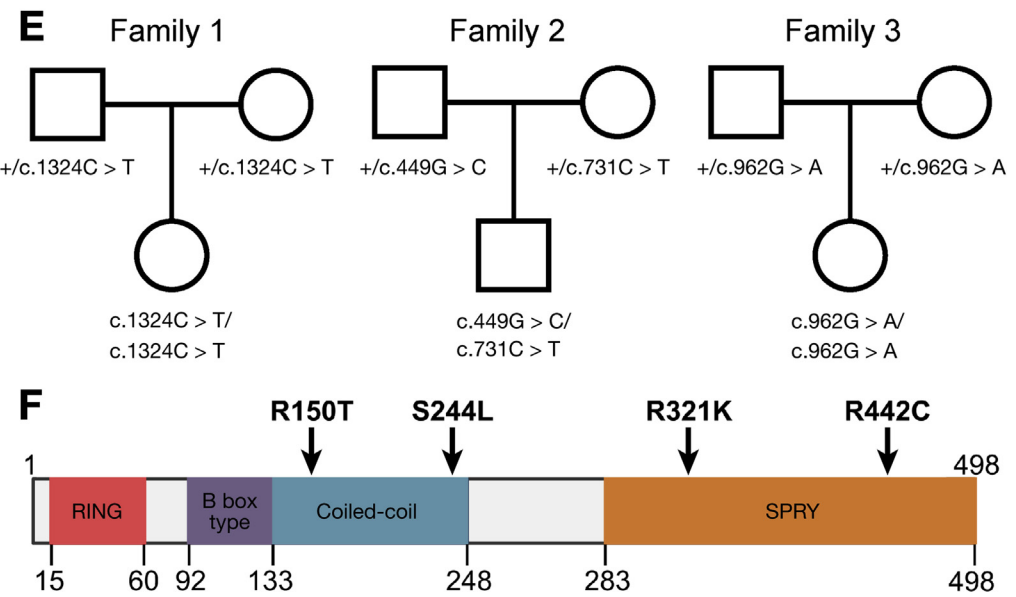


Figure 1. Clinical features and pedigrees of patients with *TRIM22* variants. (A, B) Clinical presentation and histopathologic findings in colonic biopsy from patient 1. (A) Severe perianal fistulization with seton placement. Rectovaginal fistulae were also present. (B) Non-caseating granulomas on a background of chronic inflammatory cell infiltrates (H&E stain). (C, D) Clinical presentation and histopathologic findings in colonic biopsy from patient 2. (C) Multiple, severe cavitating perianal fistulae. (D) Colonic biopsy showing chronic inflammation with non-caseating granuloma (black arrow) (H&E stain, scale bar = 75 μ m). (E) Pedigree analysis of the genetic inheritance pattern for each family trio. (F) Schematic view of the protein domain architecture of *TRIM22* with the relative position of each identified variant depicted. Number indicates amino acid position.



resulted in an arginine to lysine substitution (p.Arg321Lys; c.962G>A). The R321K variant was predicted to be deleterious and located in the highly conserved SPRY domain on an exposed residue of a beta sheet that has a functional role in the antiviral activity patch of the SPRY domain²⁷ (Figure 1F, Supplementary Table 1B).

Integrative Analysis Supports *TRIM22* as a Key Regulator in Inflammatory Bowel Disease–Associated Networks

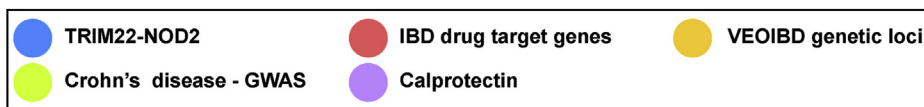
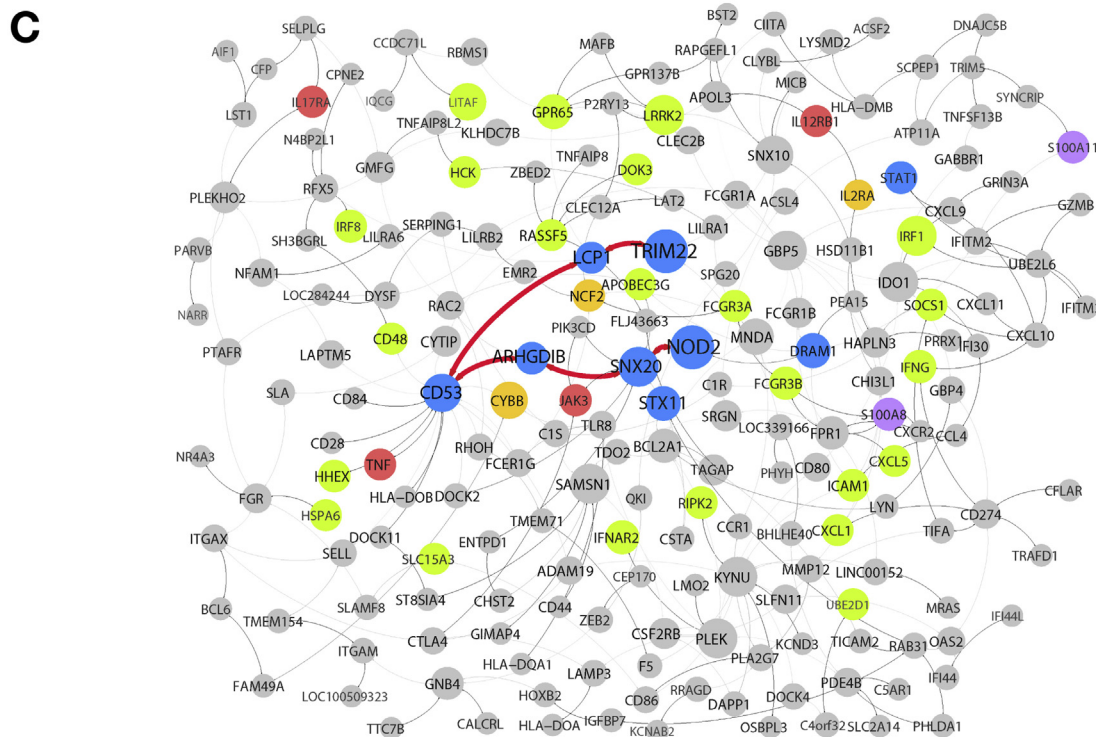
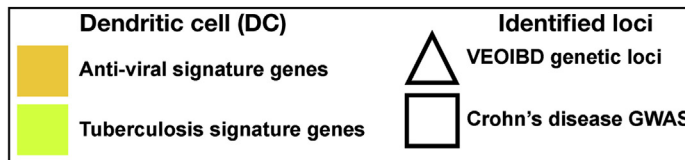
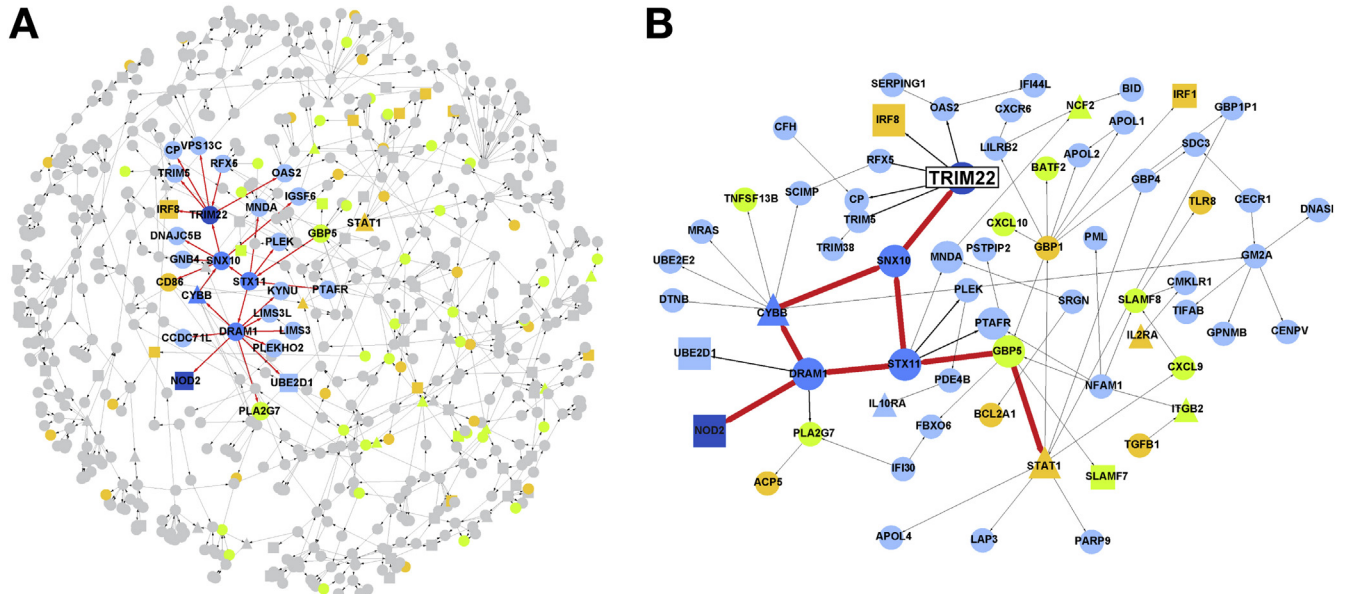
To gain insight into the role of *TRIM22* in the pathogenesis of IBD, we constructed a probabilistic causal network

model by integrating 7,568 RNA-sequence–derived gene expression traits from ileal biopsies from 322 treatment-naïve pediatric Crohn’s patients in the RISK cohort¹⁹ and eQTL. To identify the VEOIBD component of this molecular network, we projected all genes known to be causally associated with VEOIBD⁹ (Supplementary Table 3) onto this network, and then identified the most connected subnetwork containing these VEOIBD genes within the full RISK network, resulting in the VEOIBD network composed of 665 genes, which included *TRIM22* (Figure 2A).

To understand the regulation of this VEOIBD network, we employed a previously established procedure²⁶ to identify key regulator genes that are predicted to modulate the state of the

network (Supplementary Table 4). Interestingly, the most significant key regulators identified in the VEOIBD network included *SNX10*, *STX11*, *CYBB*, and *DRAM1*, which directly

connect *TRIM22* to the IBD gene *NOD2* via 2 equidistant paths. The first pathway, *TRIM22* → *SNX10* → *STX11* → *DRAM1* → *NOD2*, is linked to the known VEOIBD gene *STAT1*



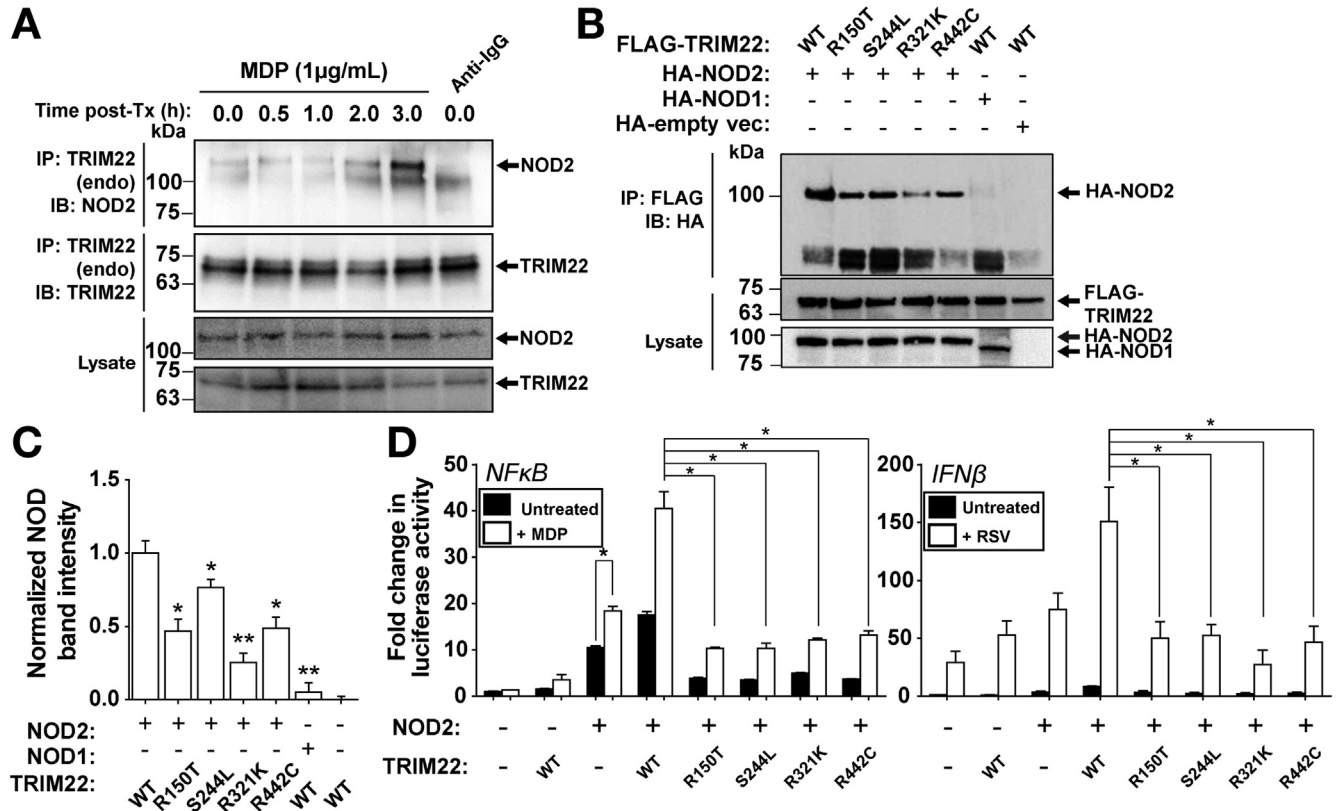


Figure 3. TRIM22 interacts with and activates NOD2 signaling. (A) Endogenous NOD2 and TRIM22 co-immunoprecipitate after MDP stimulation. HT29 cells were stimulated with MDP (1 μ g/mL) for various time periods. After treatment, cells were lysed and endogenous TRIM22 was immunoprecipitated using anti-TRIM22 antibody conjugated to Protein G-Sepharose. Bound levels of endogenous NOD2 were evaluated using Western blotting. As stimulation time with MDP increased, the binding of endogenous NOD2 to TRIM22 increased. Immunoprecipitation with IgG bound to Protein G-Sepharose was used as a negative immunoprecipitation control. (B) TRIM22 interacts with NOD2. HEK293T cells were transiently cotransfected with HA-NOD2 and either wild-type (WT) or variant (R150T, S244L, R321K, and R442C) FLAG-epitope tagged TRIM22. Twenty-four hours post transfection, cells were lysed followed by immunoprecipitation of the FLAG-TRIM22 by anti-FLAG-agarose. Reduced binding of NOD2 to TRIM22 was observed in varying degrees for each variant compared to the WT protein. HA-NOD1 and an empty vector construct were used as negative controls. (C) Quantification of NOD2 co-immunoprecipitation with WT or mutant TRIM22. Densitometry analysis was performed on Western blots performed in (B). Each TRIM22 point mutation significantly reduced NOD2 co-immunoprecipitation (Student's *t* test, **P* < .05; ***P* < .01, *n* = 3). (D) TRIM22 mutants fail to activate NF- κ B and interferon-beta downstream of NOD2. HCT116 cells were transiently co-transfected with (or without) NOD2, TRIM22-WT, or TRIM22 point mutants (R150T, S244L, R321K, R442C). Twenty-four hours post transfection, cells were stimulated with either MDP (10 μ g/mL) or RSV (0.1 μ g) for 18 hours before NF- κ B or interferon-beta promoter activation was evaluated by luciferase assay. Cells transfected with TRIM22 mutants showed significantly reduced NF- κ B and interferon-beta promoter activation after stimulation compared with WT TRIM22 transfected controls (**P* < .001 after Bonferroni post-hoc testing, *n* = 3).

via *STX11* and *GBP5*, while the second pathway, *TRIM22* \rightarrow *SNX10* \rightarrow *CYBB* \rightarrow *DRAM1* \rightarrow *NOD2*, contains the known VEOIBD gene *CYBB* (Figure 2B). Both *STAT1* and *CYBB*, in addition to *IRF8*, which is directly connected to *TRIM22*, are

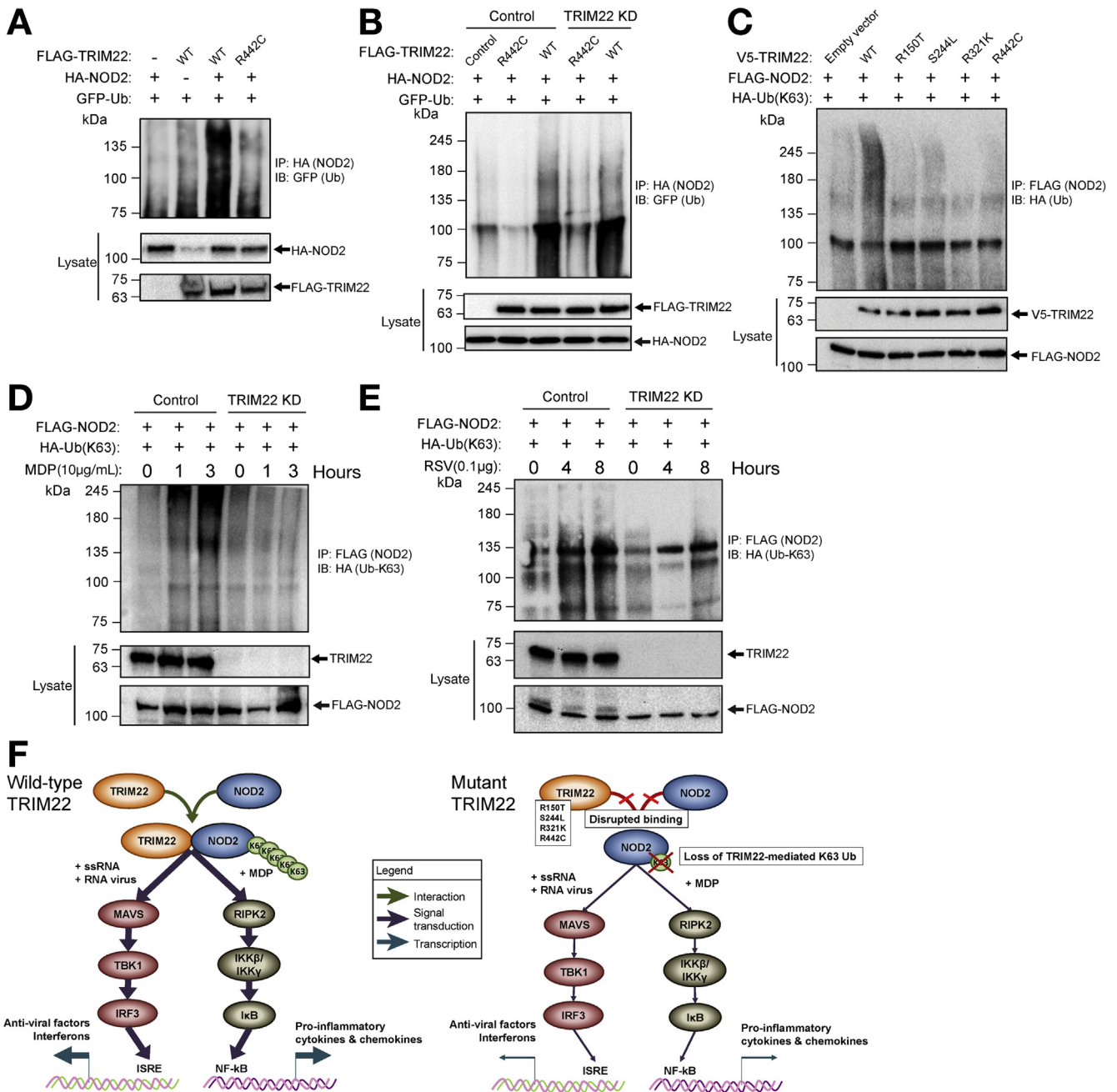
associated with Mendelian susceptibility to mycobacteria deficiency.²⁹ As expected, we did not identify any common DNA variants from the International Inflammatory Bowel Disease Genetics Consortium GWAS³⁰ within the *TRIM22* locus

Figure 2. *TRIM22*-*NOD2* network. (A) VEOIBD loci-focused subnetwork within RISK Pediatric Crohn's ileum network. To define the context of VEOIBD in the ileum network, genes known to be causally associated with VEOIBD (not including *TRIM22*) were projected onto the RISK network and extended out a path length of 2. The resulting VEOIBD focused subnetwork is composed of 665 genes and contains *TRIM22* and *NOD2*. The *TRIM22*-*NOD2* paths are highlighted in bold and are connected to the known VEOIBD loci *CYBB* and *STAT1*, as well as the GWAS locus *IRF8*. (B) Local network structure surrounding the *NOD2*/*TRIM22* paths in the 665-node VEOIBD focused subnetwork. Representative nodes from the 179-gene *TRIM22* network within the 665 node VEOIBD loci focused RISK subnetwork. (C) *TRIM22*-*NOD2* interaction is conserved in the adult IBD intestine. This network provides the context of the *TRIM22*-*NOD2* interaction in the adult IBD intestine. The 179-gene *TRIM22* network was projected and extended out an additional path length on the adult IBD pan intestine Bayesian network. IBD GWAS (green), VEOIBD loci (orange), IBD drug targets approved or in clinical development (red), and calprotectin (S100A8) (purple) are all represented in this conserved subnetwork.

(Supplementary Tables 5 and 6), however, the VEOIBD sub-network is well represented in genes involved in TRIM22-relevant pathways, including p53, ubiquitin response, and antiviral signaling, which were among the top pathways enriched for genes associated with intestine and blood eQTL that were also associated with adult IBD loci identified in the International Inflammatory Bowel Disease Genetics Consortium cohort (Supplementary Figure 3, Supplementary Table 7). In addition, we found that the VEOIBD network was 2.1-fold enriched ($P = 2.3 \times 10^{-5}$) for Crohn's genes annotated from adult IBD genetic studies that also give rise to blood eQTLs³¹ (Supplementary Table 8).

Adult-Onset Inflammatory Bowel Disease Informed by a TRIM22-Centered Network

Given preliminary support for adult IBD in the VEOIBD network, we explored whether the TRIM22 component of the VEOIBD network was associated with adult IBD. We constructed an adult IBD causal gene network from gene expression and genotype data generated on 203 intestinal biopsies, which included inflamed and noninflamed tissues from ileum, ascending colon, descending colon, transverse colon, sigmoid, and rectum. All of these tissues, in addition to blood, were collected at baseline from 54 anti-TNF α -resistant Crohn's patients enrolled in the



ustekinumab (IL12/IL23 p40 monoclonal antibody) clinical trial¹⁸ (Supplementary Figure 4). We found that *TRIM22* was not only a key driver gene in the sigmoid (key driver $p = 4.0e-06$) and rectum (key driver $P = 1.0e-4$) networks, but it was significantly upregulated in inflamed sigmoid (fold change = 2.47, SAM-based $p = 6.31e-05$) and inflamed rectum (fold change = 2.39, SAM-based $P = 5.03 e-06$), compared with non-inflamed samples of these same tissues.

We identified the homologous *TRIM22* component of the adult IBD network by first identifying all genes within a path length of 5 to *TRIM22* in the VEOIBD network, which included *NOD2*, leaving a network composed of 179 genes (referred to here as the *TRIM22* network; Supplementary Table 9). This *TRIM22* network contained many macrophage/monocyte-expressed genes associated with mycobacterial and antiviral responses (including genes involved in autophagy, NF- κ B pathway, and apoptosis; Supplementary Figure 5; Supplementary Table 10). Strikingly, of the 480 key driver genes we identified in the adult IBD network, 62, including *STX11*, *CYBB*, and *DRAM1*, were represented in the pediatric *TRIM22* network, 7.2-fold enrichment over what is expected by chance ($P = 6.5 e-38$) (Supplementary Table 11). Further, the *TRIM22* containing co-expression module from the blood of ustekinumab patients, which was 12.7-fold enriched for response to virus ($P = 6.3e-14$), was 9-fold enriched in the pediatric *TRIM22* network ($P < 1e-16$). Further supporting the pediatric *TRIM22* network's association to viral response was a 3.2-fold enrichment ($P = 2.5e-5$) of eQTLs associated with dendritic cell response to stimulation with flu or interferon beta³² and an 8.3-fold enrichment ($P = 1.1e-16$) of genes in a tuberculosis infection signature in dendritic cells.³⁰

The homologous *TRIM22* network in the adult IBD network was then identified by projecting nodes from the

TRIM22 network onto the adult IBD network, identifying those nodes that were either in the *TRIM22* network or directly connected to such nodes (Figure 2C). In this *TRIM22* pediatric-oriented adult IBD network, *TRIM22* is in close proximity to several drug targets that are either approved or in clinical development for IBD, including TNF α , the target of adalimumab (Humira), certolizumab (Cimzia), infliximab (Remicade), and colimumab (Simponi); IL12R β , a chain shared between the receptors that bind IL12/23, the molecular target of ustekinumab; JAK3, the target of tofacitinib; and IL17RA, the target of brodalumab.

Because S100A8 (calprotectin), a stool biomarker for inflammation, is also co-localized with *TRIM22* in this network³³⁻³⁵ (Figure 2C), we decided to further investigate the role of *TRIM22* in treatment-refractory patients, exploring associations between *TRIM22* and IBD-associated clinical traits in the ustekinumab clinical trial (Supplementary Table 12). We found that expression levels of *TRIM22* in the colon were positively correlated with fecal calprotectin regardless of biopsy inflammation status. Overall, both inflamed and noninflamed baseline intestine levels of *TRIM22* revealed a correlation to blood C-reactive protein, of which consistently high levels are associated with subsequent development of perianal fistulae in Crohn's patients³⁶ and response to anti-TNF α .³⁷ *TRIM22* expression levels in blood were positively correlated with Crohn's Disease Activity Index (Supplementary Table 13).

Taken together, the intestinal network models provide causal support for the *TRIM22* regulation of *NOD2* and the correlation of the *TRIM22-NOD2* pathway with predicted disease regulators, functionally relevant VEO and adult-onset IBD genetic loci, effectors of antiviral and mycobacterial function, correlation with inflammatory clinical variables and validated IBD drug targets.

Figure 4. *TRIM22* mediates K63-linked *NOD2* polyubiquitination. (A) *TRIM22* enhances *NOD2* polyubiquitination in HEK293 cells. HEK293T cells were transiently co-transfected with HA-*NOD2*, green fluorescent protein (GFP) ubiquitin, and either wild-type (WT) or variant (R442C) FLAG-*TRIM22*. Twenty-four hours post transfection, cells were lysed followed by immunoprecipitation of HA-*NOD2*. Ubiquitination of *NOD2* was evaluated by immunoblotting for GFP (ubiquitin). Co-transfection with WT *TRIM22* enhanced ubiquitination of *NOD2*, which was abrogated with the R442C variant *TRIM22*. All experiments were carried out in triplicate, independent experiments. (B) Transgenic *TRIM22* rescues *NOD2* polyubiquitination in *TRIM22*-shRNA-HT29 cells. HT29 cells stably transduced with control (scramble) or *TRIM22* short-hairpin RNA (shRNA) were transiently co-transfected with HA-*NOD2* and either WT or variant (R442C) FLAG-*TRIM22*. Twenty-four hours post transfection, cells were lysed followed by immunoprecipitation of the HA-*NOD2*. Evaluation of *NOD2* poly-ubiquitination by GFP immunoblotting demonstrated rescued ubiquitination after transfection of WT-*TRIM22* in the *TRIM22* shRNA cell line that was not observed after transfection of the variant R442C. All experiments were carried out in triplicate, independent experiments. (C) Variants in *TRIM22* abrogates K63-linked *NOD2* polyubiquitination. HEK293T cells were transiently cotransfected with FLAG-*NOD2*, HA-(K63-specific) ubiquitin, and either WT or variant (R150T, S244L, R321K, or R442C) V5-*TRIM22*. Twenty-four hours post transfection, cells were lysed followed by immunoprecipitation of the FLAG-*NOD2*. Evaluation of *NOD2* K63 specific-ubiquitination by HA immunoblotting demonstrated significantly reduced ubiquitination in cells cotransfected with *TRIM22* variants compared to WT. All experiments were carried out in triplicate, independent experiments. (D, E) *TRIM22*-shRNA reduces MDP- and RSV-induced K63-linked *NOD2* polyubiquitination. HEK293T cells stably transduced with control (scramble) or *TRIM22* shRNA were transfected with HA-tagged K63-specific ubiquitin and FLAG-*NOD2*. Forty-eight hours after transfection, cell lysates were stimulated by MDP (D) or RSV (E) for indicated the time points, followed by lysis and immunoprecipitation using anti-FLAG-agarose. K63-poly-ubiquitination of *NOD2* was evaluated by immunoblotting using anti-HA antibody. After stimulation by either MDP or RSV, *NOD2* K63-specific ubiquitination increased over treatment time. However, in *TRIM22* knockdown cells, this ubiquitination was significantly reduced or absent. All experiments were carried out in triplicate independent experiments and blots are representative. (F) Schematic overview of the proposed impact of *TRIM22* and its identified variants on the *NOD2* signaling axis. WT *TRIM22* binds and mediates the K63-specific polyubiquitination of *NOD2*, potentiating downstream signaling through the MAVS and RIPK2 signaling axes depending on antigen. *TRIM22* variants disrupt binding to *NOD2*, abrogating this polyubiquitination thus attenuating downstream pro-inflammatory signaling.

Identification of TRIM22 as a NOD2 Interacting Protein

As NOD2 signaling plays a critical role in Crohn's disease susceptibility^{38,39}; we further investigated this *in silico* TRIM22–NOD2 interaction. Immunofluorescence showed that NOD2 and TRIM22 colocalized in colonic biopsies and in the cytoplasm of transiently transfected HEK293 cells (Supplementary Figure 6A–C). This NOD2 immunostaining was blocked by a NOD2-specific peptide and TRIM22 did not colocalize with NOD1 (Supplementary Figure 6D–F), another member of the NOD family, confirming the specificity of this TRIM22–NOD2 interaction. Immunostaining of colonic biopsy samples from patients 1–3 with TRIM22 variants showed altered expression and localization of NOD2 and TRIM22 (Supplementary Figure 6A and B).

TRIM22 Influences NOD2 Signaling Pathways

NOD2 senses MDP, a conserved structure in peptidoglycan present in most Gram-negative and Gram-positive bacteria. We found that TRIM22 was weakly associated with endogenous NOD2 in coimmunoprecipitation experiments in unstimulated HT29 cells, a human intestinal epithelial cell line, and this association increased after stimulation with MDP (Figure 3A). Furthermore, transiently transfected TRIM22 and NOD2 were found to reciprocally coimmunoprecipitate and these interactions were reduced with the TRIM22 variants (Figure 3B and C and Supplementary Figure 7A).

Because TRIM22 colocalized and coimmunoprecipitated with NOD2, we next determined whether TRIM22 influenced MDP-induced NF- κ B signaling via NOD2. In reporter assays, coexpression of TRIM22 and NOD2 enhanced MDP-induced activation of the NF- κ B (Figure 3D) in HEK293 cells. As TRIM22 regulates viral activity^{15–17} and NOD2 functions as cytoplasmic viral pathogen recognition receptor by triggering interferon-beta activation in response to RSV,^{40,41} we next determined whether TRIM22 also regulated NOD2-dependent RSV-induced interferon-beta signaling. As shown in Figure 3D, overexpression of TRIM22 and NOD2 both enhanced RSV-induced activation of the interferon-beta promoter and the interferon-stimulated response element. Neither wild-type TRIM22 nor the TRIM22-R442C variant enhanced TNF α gene expression in response to TNF α (Supplementary Figure 7B). As TNF α activates NF- κ B target genes independent of NOD2 signaling,⁴² this suggested that TRIM22 regulation of MDP-induced NF- κ B activation is NOD2-dependent.

TRIM22 Variants Influence NOD2 Signaling

We next examined the role of TRIM22 to regulate NOD2-dependent NF- κ B and interferon-beta signaling. Luciferase assays using HEK293 cells and real-time polymerase chain reaction experiments using HCT116 showed that expression of wild-type TRIM22 potentiated NOD2 signaling in response to both MDP-induced NF- κ B and RSV-induced interferon-beta activation (Figures 3D and Supplementary Figures 7C–F). However, the TRIM22 variants (Figures 3D and Supplementary Figures 7C–E) and TRIM22 knockdown

using short-hairpin RNA (Supplementary Figure 8A) showed impaired NOD2-dependent NF- κ B and interferon-beta signaling (Supplementary Figure 8B). MDP-mediated NOD2-dependent signaling was also significantly reduced in patient 2 only, with the heterozygous TRIM22 variants in the coiled-coil domain (Supplementary Figure 9 and Supplementary Material). Together, these data suggest that TRIM22 is a positive regulator of antiviral and antibacterial NOD2-dependent signaling pathways.

TRIM22 Mediates K63-Linked Polyubiquitination of NOD2

As TRIM22 is a RING finger E3 ubiquitin ligase¹¹ and NOD2 has high confidence predicted ubiquitination sites at K436 and K445 (CKSAAP_UbSITE⁴³), we next determined whether TRIM22 mediated ubiquitination of NOD2. Immunoprecipitation experiments using a HEK293 cell line co-expressing HA-NOD2 and Flag-TRIM22 showed that overexpression of TRIM22 enhanced NOD2 polyubiquitination (Figure 4A). The TRIM22 variants (Figure 4A and Supplementary Figure 10A) were unable to mediate this NOD2 polyubiquitination. TRIM22 did not increase polyubiquitination of other components (MAVS or RIPK2) of the NOD2 signaling pathways known to be ubiquitinated^{44,45} (Supplementary Figure 10B). Using the TRIM22 short-hairpin RNA HT29 stable cell line, we found that only wild-type TRIM22 rescued NOD2 polyubiquitination and not the TRIM22-R442C variant (Figure 4B). Taken together, this suggested that TRIM22 specifically mediates NOD2 polyubiquitination.

K63-linked polyubiquitination regulates the localization and signaling activity, whereas K48-linked polyubiquitination often mediates degradation.⁴⁶ NOD2 has been previously shown to be K48-linked ubiquitinated by TRIM27 and results in NOD2 degradation.⁴⁷ Using ubiquitin mutants, we showed that overexpression of TRIM22 mediated K63-linked but not K48-linked polyubiquitination of NOD2, while the TRIM22 variants were unable to mediate K63- or K48-linked NOD2 polyubiquitination (Figure 4C and Supplementary Figure 11A). We next determined that TRIM22 is required for MDP- and RSV-induced K63-linked NOD2 polyubiquitination and knockdown of TRIM22 reduced this MDP- and RSV-induced K63-linked (Figure 4D and E), but not K48-linked NOD2 polyubiquitination (Supplementary Figures 11B and C).

Discussion

TRIM proteins are involved in a number of biologic processes, including cell proliferation, apoptosis, innate immunity, autoimmunity, and inflammatory response.^{48,49} Variants in TRIM genes result in monogenic diseases, including familial Mediterranean fever and Opitz syndrome type 1, and are implicated in a number of cancers and autoimmune diseases, including multiple sclerosis, rheumatoid arthritis, and systemic lupus erythematosus.^{48,49} TRIM22 belongs to a subfamily of TRIM proteins that contain a SPRY domain and are thought to have evolved to

limit innate immune responses to viruses.²⁰ Mutations in the SPRY domain of TRIM20 (pyrin) result in autoimmune diseases, including familial Mediterranean fever.⁵⁰ Overexpression of TRIM22 is known to activate NF- κ B in a dose-dependent manner and both the N-terminal RING domain and C-terminal SPRY domain are crucial for TRIM22-mediated NF- κ B activation¹³ and antiviral activity,¹⁵⁻¹⁷ and are implicated in the pathogenesis of autoimmune diseases.⁵¹ Patients 1 and 3 both had homozygous variants in the SPRY domain and patient 2 had compound heterozygous variants both predicted to disrupt the coiled-coil domain and had loss of NOD2-dependent MDP signaling. The characterized *TRIM22* variants resulted in impaired NOD2 binding and K63-linked NOD2 polyubiquitination. The predicted NOD2 polyubiquitination sites described earlier are in the NACHT domain, a conserved domain required for NOD2 conformational change in response to MDP sensing through the LRR domain or interaction with binding adaptor proteins for NOD2.⁵² Therefore, as all identified *TRIM22* variants disrupt both NOD2-dependent NF- κ B and interferon-beta signaling, this suggests that K63-linked polyubiquitination of NOD2 mediated by TRIM22 is critical for NOD2 function (Figure 4F).

NOD2 has long been recognized as a critical player in Crohn's disease pathogenesis,^{38,39} where it is proposed to regulate innate immunity through NF- κ B–induced pro-inflammatory responses triggered by peptidoglycan (reviewed in Shaw et al⁵³). Numerous studies have shown that the loss of function variants in NOD2 associated with Crohn's disease result in the loss of NF- κ B–induced pro-inflammatory cytokine response to MDP (reviewed in Strober et al⁵⁴ and Philpott et al⁵⁵) and, therefore, mirror the defect we observe in patient 2 with TRIM22 mutations in the coiled-coil domain. Similarly, mutations in XIAP (also an E3 ubiquitin ligase) are associated with IBD with granulomatous colitis and perianal disease^{56,57} and are associated with loss of NOD2-dependent mediated NF- κ B signaling⁵⁸⁻⁶⁰ and XIAP is also regulated by TRIM proteins.⁶¹ XIAP deficiency usually presents in early childhood, but there are cases of patients presenting with IBD at older than 40 years of age⁹ with and without hemophagocytic lymphohistiocytosis (reviewed in Latour and Aguilar⁶²). Furthermore, XIAP not only regulates NOD2-dependent innate immunity responses, but also is proposed to regulate inflammasome and adaptive immunity.⁶² Loss-of-function NOD2 variants associated with IBD have low penetrance and do not cause the severe early-onset disease observed in this group with either TRIM22 or XIAP deficiency. Therefore, it is most likely that, in patients 1 and 3 with TRIM22 SPRY domain variants, defects in other pathways regulated by TRIM22 result in the early onset and severity of disease. Alternatively, hypomorphic TRIM22 variants act in an oligogenic manner with mutations in other genes similar to what has been observed with hypomorphic XIAP mutations⁶³ and as observed in patient 3, who is also a carrier of a XIAP mutation. Together, this suggests that loss of NOD2-dependent–mediated signaling in response to MDP contributes to a severe form of IBD and that other yet defined pathways must also be involved in disease

pathogenesis. With regard to TRIM22 specifically, we anticipate that other pathways not identified in these studies play a role in disease pathogenesis.

Our computational studies further support our functional studies demonstrating that TRIM22 influences both NOD2-dependent interferon-beta and NF- κ B signaling pathways. Although the loss-of-function *TRIM22* variants in our VEOIBD patients can manifest as an immunodeficiency, the inflammation and tissue damage that ensues from a dysregulated response to microbial burden might resemble the profile of adult-onset IBD. The functional outcome of pro-inflammatory NF- κ B activation may differ, depending on the cell population in which TRIM22 is expressed, with circulating plasmacytoid dendritic cells and monocytes predominating in the blood and resident intestinal dendritic cells, macrophages, and enterocytes in the intestine. We see from the intestine network that the regulation of causal TRIM22 results in modulation of a mycobacterial and viral response subnetwork that can also result in feedback to TRIM22 expression. Either due to immunodeficiency arising from the *TRIM22* variants or excessive inflammation in non-*TRIM22* variants carried by anti-TNF α refractory patients, TRIM22-driven NOD2 activation in response to MDP or viral stimuli, contributes to dysregulation of NF- κ B– and interferon-beta–driven pathways as reflected in the networks. Together, this demonstrates that the *TRIM22-NOD2* network plays a critical role in the development of IBD.

Investigation of VEO and adult-onset IBD in treatment refractory disease will elucidate new treatment opportunities by revealing complexity of disease network dysregulation. Causal- and correlative-based network analysis allows for consideration of the synergistic effects between genes in disease, which can be a greater determinant than evaluation of single target genes to inform disease drivers and opportunities for combinatorial therapy. Network analysis can be focused by novel variants, as seen with *TRIM22* identified through WES in VEOIBD patients to generate hypothesis and potentially identify biomarkers and guide drug discovery and repositioning in both VEO and adult-onset IBD patient subsets.

Supplementary Material

Note: To access the supplementary material accompanying this article, visit the online version of *Gastroenterology* at www.gastrojournal.org, and at <http://dx.doi.org/10.1053/j.gastro.2016.01.031>.

References

1. Avitzur Y, Guo C, Mastropaolo LA, et al. Mutations in tetratricopeptide repeat domain 7A result in a severe form of very early onset inflammatory bowel disease. *Gastroenterology* 2014;146:1028–1039.
2. Elkadri A, Thoani C, Deharvengt SJ, et al. Mutations in plasmalemma vesicle associated protein result in sieving protein-losing enteropathy characterized by hypoproteinemia, hypoalbuminemia, and hypertriglyceridemia. *Cell Mol Gastroenterol Hepatol* 2015;1:381–394 e7.

3. Janecke AR, Heinz-Erian P, Yin J, et al. Reduced sodium/proton exchanger NHE3 activity causes congenital sodium diarrhea. *Hum Mol Genet* 2015;24:6614–6623.
4. Dhillon SS, Fattouh R, Elkadri A, et al. Variants in nicotinamide adenine dinucleotide phosphate oxidase complex components determine susceptibility to very early onset inflammatory bowel disease. *Gastroenterology* 2014;147:680–689 e2.
5. Dhillon SS, Mastropaolo LA, Murchie R, et al. Higher activity of the inducible nitric oxide synthase contributes to very early onset inflammatory bowel disease. *Clin Transl Gastroenterol* 2014;5:e46.
6. Moran CJ, Walters TD, Guo CH, et al. IL-10R polymorphisms are associated with very-early-onset ulcerative colitis. *Inflamm Bowel Dis* 2013;19:115–123.
7. Muise AM, Walters T, Xu W, et al. Single nucleotide polymorphisms that increase expression of the guanosine triphosphatase RAC1 are associated with ulcerative colitis. *Gastroenterology* 2011;141:633–641.
8. Muise AM, Xu W, Guo CH, et al. NADPH oxidase complex and IBD candidate gene studies: identification of a rare variant in NCF2 that results in reduced binding to RAC2. *Gut* 2012;61:1028–1035.
9. Uhlig HH, Schwerd T, Koletzko S, et al. The diagnostic approach to monogenic very early onset inflammatory bowel disease. *Gastroenterology* 2014;147:990–1007.e3.
10. **Glocker EO, Kotlarz D, Boztug K**, et al. Inflammatory bowel disease and mutations affecting the interleukin-10 receptor. *N Engl J Med* 2009;361:2033–2045.
11. **Duan Z, Gao B**, Xu W, et al. Identification of TRIM22 as a RING finger E3 ubiquitin ligase. *Biochem Biophys Res Commun* 2008;374:502–506.
12. Sawyer SL, Emerman M, Malik HS. Discordant evolution of the adjacent antiretroviral genes TRIM22 and TRIM5 in mammals. *PLoS Pathog* 2007;3:e197.
13. **Yu S, Gao B**, Duan Z, et al. Identification of tripartite motif-containing 22 (TRIM22) as a novel NF-kappaB activator. *Biochem Biophys Res Commun* 2011;410:247–251.
14. Obad S, Olofsson T, Mechti N, et al. Expression of the IFN-inducible p53-target gene TRIM22 is down-regulated during erythroid differentiation of human bone marrow. *Leuk Res* 2007;31:995–1001.
15. Barr SD, Smiley JR, Bushman FD. The interferon response inhibits HIV particle production by induction of TRIM22. *PLoS Pathog* 2008;4:e1000007.
16. Eldin P, Papon L, Oteiza A, et al. TRIM22 E3 ubiquitin ligase activity is required to mediate antiviral activity against encephalomyocarditis virus. *J Gen Virol* 2009;90:536–545.
17. **Di Pietro A, Kajaste-Rudnitski A**, Oteiza A, et al. TRIM22 inhibits influenza A virus infection by targeting the viral nucleoprotein for degradation. *J Virol* 2013;87:4523–4533.
18. Sandborn WJ, Gasink C, Gao LL, et al. Ustekinumab induction and maintenance therapy in refractory Crohn's disease. *N Engl J Med* 2012;367:1519–1528.
19. Haberman Y, Tickle TL, Dexheimer PJ, et al. Pediatric Crohn disease patients exhibit specific ileal transcriptome and microbiome signature. *J Clin Invest* 2014;124:3617–3633.
20. Tusher VG, Tibshirani R, Chu G. Significance analysis of microarrays applied to the ionizing radiation response. *Proc Natl Acad Sci U S A* 2001;98:5116–5121.
21. Madigan D, York J. Bayesian graphical models for discrete data. *International Statistical Review* 1995;63:215–232.
22. **Schadt EE, Molony C, Chudin E**, et al. Mapping the genetic architecture of gene expression in human liver. *PLoS Biol* 2008;6:e107.
23. Tran LM, Zhang B, Zhang Z, et al. Inferring causal genomic alterations in breast cancer using gene expression data. *BMC Syst Biol* 2011;5:121.
24. **Wang IM, Zhang B, Yang X**, et al. Systems analysis of eleven rodent disease models reveals an inflammatory signature and key drivers. *Mol Syst Biol* 2012;8:594.
25. Yang X, Zhang B, Molony C, et al. Systematic genetic and genomic analysis of cytochrome P450 enzyme activities in human liver. *Genome Res* 2010;20:1020–1036.
26. Zhang B, Gaiteri C, Bodea LG, et al. Integrated systems approach identifies genetic nodes and networks in late-onset Alzheimer's disease. *Cell* 2013;153:707–720.
27. Kelly JN, Barr SD. In silico analysis of functional single nucleotide polymorphisms in the human TRIM22 gene. *PLoS One* 2014;9:e101436.
28. Herr AM, Dressel R, Walter L. Different subcellular localisations of TRIM22 suggest species-specific function. *Immunogenetics* 2009;61:271–280.
29. Bustamante J, Boisson-Dupuis S, Abel L, et al. Mendelian susceptibility to mycobacterial disease: genetic, immunological, and clinical features of inborn errors of IFN-gamma immunity. *Semin Immunol* 2014;26:454–470.
30. Jostins L, Ripke S, Weersma RK, et al. Host-microbe interactions have shaped the genetic architecture of inflammatory bowel disease. *Nature* 2012;491:119–124.
31. **Westra HJ, Peters MJ**, Esko T, et al. Systematic identification of trans eQTLs as putative drivers of known disease associations. *Nat Genet* 2013;45:1238–1243.
32. **Lee MN, Ye C**, Villani AC, et al. Common genetic variants modulate pathogen-sensing responses in human dendritic cells. *Science* 2014;343:1246980.
33. Sandborn WJ, Ghosh S, Panes J, et al. Tofacitinib, an oral Janus kinase inhibitor, in active ulcerative colitis. *N Engl J Med* 2012;367:616–624.
34. Ho GT, Lee HM, Brydon G, et al. Fecal calprotectin predicts the clinical course of acute severe ulcerative colitis. *Am J Gastroenterol* 2009;104:673–678.
35. Leach ST, Yang Z, Messina I, et al. Serum and mucosal S100 proteins, calprotectin (S100A8/S100A9) and S100A12, are elevated at diagnosis in children with inflammatory bowel disease. *Scand J Gastroenterol* 2007;42:1321–1331.
36. Radford Smith G, Ferguson E, Hanigan K, et al. P226. Consistently high C reactive protein is associated with subsequent development of perianal fistulae in patients with Crohn's disease. *J Crohns Colitis* 2015;9(Suppl 1):S188.
37. **Murdoch T, O'Donnell S**, Silverberg MS, et al. Biomarkers as potential treatment targets in inflammatory

- bowel disease: a systematic review. *Can J Gastroenterol Hepatol* 2015;29:203–208.
38. Hugot JP, Chamaillard M, Zouali H, et al. Association of NOD2 leucine-rich repeat variants with susceptibility to Crohn's disease. *Nature* 2001;411:599–603.
 39. Ogura Y, Bonen DK, Inohara N, et al. A frameshift mutation in NOD2 associated with susceptibility to Crohn's disease. *Nature* 2001;411:603–606.
 40. Kim YG, Park JH, Reimer T, et al. Viral infection augments Nod1/2 signaling to potentiate lethality associated with secondary bacterial infections. *Cell Host Microbe* 2011;9:496–507.
 41. Sabbah A, Chang TH, Harnack R, et al. Activation of innate immune antiviral responses by Nod2. *Nat Immunol* 2009;10:1073–1080.
 42. Li Q, Verma IM. NF-kappaB regulation in the immune system. *Nat Rev Immunol* 2002;2:725–734.
 43. Chen Z, Chen YZ, Wang XF, et al. Prediction of ubiquitination sites by using the composition of k-spaced amino acid pairs. *PLoS One* 2011;6:e22930.
 44. Castanier C, Zemirli N, Portier A, et al. MAVS ubiquitination by the E3 ligase TRIM25 and degradation by the proteasome is involved in type I interferon production after activation of the antiviral RIG-I-like receptors. *BMC Biol* 2012;10:44.
 45. Yang S, Wang B, Humphries F, et al. Pellino3 ubiquitinates RIP2 and mediates Nod2-induced signaling and protective effects in colitis. *Nat Immunol* 2013;14:927–936.
 46. **Walczak H, Iwai K, Dikic I.** Generation and physiological roles of linear ubiquitin chains. *BMC Biol* 2012;10:23.
 47. Zurek B, Schoultz I, Neerincx A, et al. TRIM27 negatively regulates NOD2 by ubiquitination and proteasomal degradation. *PLoS One* 2012;7:e41255.
 48. Jefferies C, Wynne C, Higgs R. Antiviral TRIMs: friend or foe in autoimmune and autoinflammatory disease? *Nat Rev Immunol* 2011;11:617–625.
 49. **Kawai T, Akira S.** Regulation of innate immune signalling pathways by the tripartite motif (TRIM) family proteins. *EMBO Mol Med* 2011;3:513–527.
 50. Chae JJ, Wood G, Masters SL, et al. The B30.2 domain of pyrin, the familial Mediterranean fever protein, interacts directly with caspase-1 to modulate IL-1beta production. *Proc Natl Acad Sci U S A* 2006;103:9982–9987.
 51. Hattlmann CJ, Kelly JN, Barr SD. TRIM22: a diverse and dynamic antiviral protein. *Mol Biol Int* 2012;2012:153415.
 52. Zurek B, Proell M, Wagner RN, et al. Mutational analysis of human NOD1 and NOD2 NACHT domains reveals different modes of activation. *Innate Immun* 2012;18:100–111.
 53. Shaw MH, Kamada N, Warner N, et al. The ever-expanding function of NOD2: autophagy, viral recognition, and T cell activation. *Trends Immunol* 2011;32:73–79.
 54. Strober W, Watanabe T. NOD2, an intracellular innate immune sensor involved in host defense and Crohn's disease. *Mucosal Immunol* 2011;4:484495.
 55. Philpott DJ, Sorbara MT, Robertson SJ, et al. NOD proteins: regulators of inflammation in health and disease. *Nat Rev Immunol* 2014;14:9–23.
 56. Marsh RA, Rao K, Satwani P, et al. Allogeneic hematopoietic cell transplantation for XIAP deficiency: an international survey reveals poor outcomes. *Blood* 2013;121:877–883.
 57. Zeissig Y, Petersen BS, Milutinovic S, et al. XIAP variants in male Crohn's disease. *Gut* 2015;64:66–76.
 58. Abbott DW, Yang Y, Hutti JE, et al. Coordinated regulation of Toll-like receptor and NOD2 signaling by K63-linked polyubiquitin chains. *Mol Cell Biol* 2007;27:6012–6025.
 59. **Damgaard RB, Fiil BK, Speckmann C, et al.** Disease-causing mutations in the XIAP BIR2 domain impair NOD2-dependent immune signalling. *EMBO Mol Med* 2013;5:1278–1295.
 60. Krieg A, Correa RG, Garrison JB, et al. XIAP mediates NOD signaling via interaction with RIP2. *Proc Natl Acad Sci U S A* 2009;106:14524–14529.
 61. **Ryu YS, Lee Y, Lee KW, et al.** TRIM32 protein sensitizes cells to tumor necrosis factor (TNFalpha)-induced apoptosis via its RING domain-dependent E3 ligase activity against X-linked inhibitor of apoptosis (XIAP). *J Biol Chem* 2011;286:25729–25738.
 62. Latour S, Aguilar C. XIAP deficiency syndrome in humans. *Semin Cell Dev Biol* 2015;39:115–123.
 63. Rigaud S, Lopez-Granados E, Siberil S, et al. Human X-linked variable immunodeficiency caused by a hypomorphic mutation in XIAP in association with a rare polymorphism in CD40LG. *Blood* 2011;118:252–261.

Author names in bold designate shared co-first authorship.

Received September 25, 2015. Accepted January 22, 2016.

Reprint requests

Address requests for reprints to: Aleixo Muise, MD, PhD, The Hospital for Sick Children, 555 University Avenue, Toronto, Ontario M5G 1X8, Canada. e-mail: aleixo.muise@utoronto.ca; fax: (416) 813-6531.

Acknowledgments

The authors thank the patients and their families described here from Canada and Australia. The authors thank Karoline Fielder and Dr. Amanda Charlton for assistance with patient-related materials. Thanks to Neil Warner for critical reading of the manuscript.

Lucas A. Mastropaolo, Cornelia Thoeni, Abdul Elkadri, and Tobias Schwerd contributed equally. Eric E. Schadt and Aleixo M. Muise contributed equally.

The current affiliation for Ralph Nanan, Brigitte Snanter-Nanan and Mingjing Hu is Charles Perkins Centre Nepean, The University of Sydney, Sydney Australia.

Conflicts of interest

The authors disclose no conflicts.

Funding

Christoph Klein and Daniel Kotlarz were supported by the Deutsche Forschungsgemeinschaft (SFB1054) and BioSysNe. Holm H. Uhlig is supported by the Crohn's & Colitis Foundation of America (CCFA). Tobias Schwerd is supported by the Deutsche Forschungsgemeinschaft (SCHW1730/1-1). Qi Li and Abdul Elkadri are supported by a Crohn's and Colitis Canada (CCC), Canadian Association of Gastroenterology (CAG), and Canadian Institute of Health Research (CIHR) Fellowship. Aleixo M. Muise is funded by a CIHR-operating grant (MOP119457) and Aleixo M. Muise, Christoph Klein, Scott B. Snapper, Eric E. Schadt, and Holm H. Uhlig are funded by the Leona M. and Harry B. Helmsley Charitable Trust to study VEOIBD.